

Brief Report

# The Novel Yeast PAS Kinase Rim15 Orchestrates $G_0$ -Associated Antioxidant Defense Mechanisms

Elisabetta Cameroni<sup>1,†</sup>

Nicolas Hulo<sup>2,†</sup>

Johnny Roosen<sup>3,†</sup>

Joris Winderickx<sup>3</sup>

Claudio De Virgilio<sup>1,\*</sup>

<sup>1</sup>Department of Microbiology and Molecular Medicine; <sup>2</sup>Swiss Institute of Bioinformatics; Centre Médical Universitaire; University of Geneva; Geneva, Switzerland

<sup>3</sup>Functional Biology; Katholieke Universiteit Leuven; Flanders, Belgium

<sup>†</sup>These authors contributed equally.

\*Correspondence to: Claudio De Virgilio; Department of Microbiology and Molecular Medicine; Centre Médical Universitaire; 1 rue Michel Servet; 1211 Geneva 4, Switzerland; Tel.: +41.22.379.54.95; Fax: +41.22.379.55.02; Email: Claudio.DeVirgilio@medecine.unige.ch

Received 01/30/04; Accepted 02/03/04

Previously published online as a *Cell Cycle* E-publication:  
<http://www.landesbioscience.com/journals/cc/abstract.php?id=791>

## KEY WORDS

Rim15, PAS kinase, TOR, PKA,  $G_0$ , chronological life span

## ACKNOWLEDGEMENTS

This work was supported by grants from the Katholieke Universiteit Leuven and the Fund for Scientific Research of Flanders to J.W. and the Swiss National Science Foundation to C.D.V. (631-62731.00).

We are grateful to Costa Georgopoulos for critically reading the manuscript.

## ABSTRACT

The highly conserved PKA and TOR proteins define key signaling pathways that control cell proliferation in response to growth factors and/or nutrients. In yeast, inactivation of PKA and/or TOR causes cells to arrest growth in early  $G_1$  and induces a program that is characteristic of  $G_0$  cells. We have recently shown that the protein kinase Rim15 integrates both PKA- and TOR-mediated signals. In this work, we demonstrate that the Rim15-activated genomic expression program following glucose limitation at the diauxic shift is mediated by the three transcription factors Gis1, Msn2, and Msn4. The Rim15 regulon comprises several gene clusters implicated in the adaptation to respiratory growth, including classical oxidative stress genes such as *SOD1* and *SOD2*, suggesting that the reduced life span of *rim15Δ* cells may be due to their deficiency in oxidative damage prevention. Interestingly, we found that the primary amino acid sequence of Rim15 includes in its amino-terminal part a conserved PAS domain, known to act as a sensor for a variety of stimuli. We propose that Rim15 has evolved to integrate nutrient signals (transduced via TOR and PKA) and redox and/or oxidative stress signals to appropriately induce a transcriptional program that ensures survival in  $G_0$ .

## INTRODUCTION

Eukaryotic cell proliferation is controlled by growth factors, hormones, and/or the availability of nutrients. In the absence of a corresponding proliferation signal, cells may enter into a specific, nondividing resting state termed stationary phase or  $G_0$ , generally associated with increased resistance to various environmental stresses. Defects in the regulatory mechanisms that control entry into or exit from  $G_0$  result in either cellular transformation (in multicellular organisms), or dramatically reduced life span (particularly of unicellular organisms). In the yeast *Saccharomyces cerevisiae*,  $G_0$  entry is primarily regulated by the availability of nutrients and, in cells grown on rich glucose-containing medium, results from progression through distinct adaptive phases, which critically affect the cell's life span or their ability to withstand environmental stresses.<sup>1-4</sup> The earliest of these phases begins when about half of the initial glucose is exhausted and is characterized by the onset of glycogen synthesis.<sup>5</sup> Subsequent phases, which are critical for the development of stress resistance, include induction of stress-responsive element (STRE) and post-diauxic shift (PDS) element-controlled genes prior to and at the time of glucose exhaustion, respectively, as well as the synthesis of trehalose immediately following glucose exhaustion.<sup>5-10</sup> In the diauxic shift phase (following glucose depletion), the cells transiently reduce their growth rate to readjust their metabolism for the subsequent period of slow, respiratory growth (termed post-diauxic phase) on nonfermentable carbon sources, such as ethanol and acetate. The processes that are triggered at the diauxic transition include mainly the transcriptional induction of genes whose products are involved in respiration, fatty acid metabolism, and the glyoxylate cycle, and, possibly as a consequence of the on-setting respiratory activity, of genes encoding antioxidant defenses that allow scavenging and/or destruction of reactive oxygen species.<sup>11,12</sup> While many of these transcriptional changes persist through the post-diauxic phase, entry into  $G_0$  is ultimately characterized by strong repression of the genes devoted to protein synthesis, as well as the induction of specific late stationary phase genes (e.g., *SNZI* and *SNOI*).<sup>1,2,13,14</sup> Taken together, the final characteristics of  $G_0$  cells reflect the integration of responses and adaptations that are triggered by progression through distinct, sequential physiological phases.

The PKA and TOR signaling pathways, which positively regulate cell proliferation in response to nutrient availability, are key determinants of proper entry into  $G_0$ .<sup>1-3,9,15,16</sup>

Inactivation of either of these major pathways results in G<sub>0</sub>-like arrest, even in the presence of abundant nutrients. This observation raises the intriguing possibility that the two signaling pathways may regulate each other at some level or share a common downstream effector(s), which integrates signals from both pathways. In this context, two recent studies have shed new light on the mechanisms that allow cells to coordinate the signal flow through both pathways.

The first study expands previous knowledge on the PKA target Rim15, which has been shown to function as an activator of several essential aspects of the G<sub>0</sub> program (including proper G<sub>1</sub> cell cycle arrest, synthesis of glycogen and trehalose, and activation of Gis1-dependent, PDS-element driven transcription), and which is required for long-term postdiauxic/stationary phase survival (also referred to as chronological life span).<sup>17,18</sup> Accordingly, induction of Rim15-dependent G<sub>0</sub> traits was shown to require two discrete processes, namely, nuclear accumulation of Rim15, which appears to be negatively regulated by a Sit4-independent, rapamycin-sensitive TOR effector branch, and release from PKA-mediated inhibition of its protein kinase activity. Thus, Rim15 not only defines a new TOR effector branch that controls entry into G<sub>0</sub>, but also represents a point of convergence of the PKA and TOR nutrient signaling pathways. The PKA and TOR pathways have previously been found to signal in parallel to the partially redundant Zn<sup>2+</sup>-finger transcription factors Msn2 and Msn4, which are known to regulate STRE dependent transcription in response to a wide range of stresses (including nutrient limitation).<sup>6,7,10,19</sup> A general theme that emerges from these observations is that TOR negatively controls nuclear accumulation of PKA targets, such as Msn2 and Rim15. Thus, it will be interesting to determine whether TOR controls cytoplasmic retention and/or nuclear exclusion of the corresponding proteins via a common mechanism.

The second study provides an important clue as to how the PKA and TOR pathways may coordinately regulate G<sub>0</sub> entry by showing that inactivation of TOR causes nuclear accumulation of Tpk1,<sup>20</sup> which represents one of the three partially redundant catalytic PKA subunits. Notably, the cytoplasm of exponentially growing cells contains low levels of the PKA regulatory Bcy1 subunit, and hence primarily free, active PKA, while the inactive PKA/Bcy1 holoenzyme appears to reside predominantly in the nucleus.<sup>21</sup> Inactivation of TOR is therefore likely to result in inhibition of PKA by promoting nuclear Tpk1/Bcy1 complex formation. Taken together, relocation of PKA targets into a presumably low PKA environment (i.e., from the cytoplasm into the nucleus), as well as inactivation of PKA itself, may be complementary mechanisms that ensure proper G<sub>0</sub> entry following inactivation of TOR.

Given the key regulatory role of Rim15 for proper entry into G<sub>0</sub>, which vitally affects the organism's life span, we defined in more detail the Rim15-controlled processes by studying the genome-wide expression profile of wild-type and *rim15Δ* mutant cells. We show that Rim15 is required for transcriptional induction at the diauxic shift of several gene clusters that are implicated in the adaptation to respiratory growth. Moreover, our genome-wide expression analyses of *gis1Δ* and *msn2 msn4* mutants indicate that the transcription factors Gis1 and Msn2/4 cooperatively mediate the entire Rim15-dependent transcriptional response at the diauxic shift. We discuss these results in the context of the recent findings that life-span extension depends critically on the presence of Rim15, Msn2/4, and antioxidant defense enzymes. Finally, we present the intriguing finding that the primary amino acid sequence of Rim15 specifies in its amino-terminal part an evolutionarily conserved PAS domain, which generally act as

sensors for a variety of stimuli, including redox state, oxygen and overall cellular energy level.<sup>22,23</sup> Rim15 therefore represents a new, distinct member of the PAS kinase family that may, as suggested for other members of this family,<sup>24-26</sup> be subjected to control by its *cis* regulatory PAS domain.

## MATERIALS AND METHODS

**Yeast Strains and Media.** *S. cerevisiae* strains PEY78 (*msn2 msn4*), CDV115 (*rim15Δ*), and their wild-type parent W303-1A, as well as IP31 (*rim15Δ*) and its wild-type parent KT1960 have been described previously.<sup>27,28</sup> The *gis1Δ* mutant strain CDV116 was created by PCR-based gene deletion<sup>29</sup> (using a *gis1Δ::kanMX2* deletion cassette) of the wild-type *GIS1* copy in W303-1A. Strains were grown at 30°C in standard rich medium (YPD) with 2% glucose.<sup>30</sup>

**mRNA Preparation and Synthesis of cDNA.** Yeast strains were grown at 30°C in YPD medium. Overnight cultures of 5 ml were diluted to an OD<sub>600</sub> of 0.2 and maintained in exponential growth phase (OD<sub>600</sub> < 1.0) for a period of 24 hours by repeated dilution in fresh YPD medium to ensure complete depletion of stationary phase-specific transcripts. At this point exponential phase samples were harvested. Subsequently, the cultures were grown until glucose was exhausted, and diauxic shift samples were harvested 30 minutes after glucose exhaustion. Total RNA was then extracted using the RNeasy<sup>TM</sup> kit (Qiagen) according to the manufacturer's instructions. Radiolabeled cDNA probes were generated from 1 μg of total RNA by reverse transcription of mRNA using Superscript II (Invitrogen), an oligo(dT) primer (10-20-mer mixture; Research Genetics), and (α-<sup>32</sup>P)dCTP. Labeled probes were purified by passage through Bio-Spin 6 chromatography columns (Bio-Rad) and denatured for 5 min at 95°C.

**GeneFilter Hybridization and Data Analysis.** Yeast Index GeneFilters<sup>®</sup> (Research Genetics; Invitrogen) were hybridized with the labeled probes according to the manufacturer's protocol. The filters were scanned by a PhosphorImager (Fuji BAS-1000) to obtain digital images. Images produced by MacBas<sup>®</sup> (Fuji) were converted to TIFF and imported into the Pathways<sup>®</sup> 4.0 software (Research Genetics) for subsequent normalization against all data points and quantification of spot intensities. The average ratio was calculated from log<sub>2</sub> expression ratios during the exponential phase of growth relative to the diauxic shift transition from two independent experiments, using either wild-type or mutant strains. Noninterpretable spots were manually flagged and excluded. Ratios from duplicate experiments were averaged, and values with a standard deviation/average value of >0.5 were ignored for further analysis. The remaining 4605 open reading frames (ORFs) gave highly reproducible results. Those ORFs, whose average fold induction was higher than 2.0 in wild-type and not higher than 1.5 in *rim15Δ*, *msn2 msn4*, and *gis1Δ* cells were deemed to be significantly dependent on Rim15, Msn2/4, and Gis1, respectively, for induction at the diauxic shift. Descriptions of gene products were derived from the *Saccharomyces* Genome Database and/or the Comprehensive Yeast Genome Database (MIPS). Original data are available upon request.

**Northern Blot Analyses.** Cells were grown to early logarithmic phase at 30°C and culture aliquots were removed at the times (or glucose concentrations) indicated. Northern blot analysis was performed as previously described using PCR products (~1 kilobase) and the Prime-It Random Primer Labeling Kit (Stratagene).<sup>18</sup>

**Sequence Analyses.** Iterative database searches using profiles were performed on the nonredundant database Swiss-Prot/TrEMBL for detection of PAS domains in Rim15 and Rim15 homologues. The default parameters of the pftools and the HMMER packages were used for the construction of profiles. The graphical representation of Rim15 was adapted from the PROSITE domain visualizer ([www.expasy.org/cgi-bin/PSView/PSView.cgi?spac=P43565](http://www.expasy.org/cgi-bin/PSView/PSView.cgi?spac=P43565)).

Table 1 RIM15-DEPENDENT TRANSCRIPTION AT THE DIAUXIC TRANSITION<sup>a</sup>

Yeast	Gene	Description	Average Fold Change				STRE	PDS
			WT	<i>rim15</i> Δ	<i>msn2/msn4</i>	<i>gis1</i> Δ		
<b>Carbohydrate metabolism</b>								
YGR248W	<i>SOL4</i>	6-phosphogluconolactonase	3.84	1.35	2.14	3.91	1	2
YBR241C		Hexose transporter family member	3.76	1.45	-1.19	1.39	0	1
YIR036C		Similarity to oxidoreductases	3.21	-1.78	1.34	1.21	1	1
YOL157C		Putative alpha-glucosidase	2.84	1.44	1.25	1.60	1	1
YDL174C	<i>DLD1</i>	D-lactate dehydrogenase activity	2.81	1.22	-1.18	-1.01	1	0
YNL037C	<i>IDH1</i>	Isocitrate dehydrogenase	2.70	1.33	1.33	1.13	2	0
YPL262W	<i>FUM1</i>	Fumarate hydratase	2.64	1.12	1.12	1.92	2	0
YGR193C	<i>PDX1</i>	Pyruvate dehydrogenase complex	2.31	-1.15	1.00	1.21	2	0
YNR072W	<i>HXT17</i>	Hexose transporter	2.25	1.18	-1.03	-1.07	1	0
YDR001C	<i>NTH1</i>	Neutral trehalase	2.18	1.27	-1.03	1.71	3	0
YDR387C		Hexose transporter family member	2.12	1.24	1.48	1.25	0	0
YGL104C		Hexose transporter family member	2.11	1.18	-1.04	1.17	1	0
YIL154C	<i>IMP2'</i>	Transcription factor	2.11	1.31	-1.17	1.14	1	0
YPR006C	<i>ICL2</i>	Isocitrate lyase	2.07	1.27	1.83	1.58	0	1
YBR056W		Similarity to glucan-1,3 β-glucosidases	2.06	1.30	-1.51	1.09	1	0
YPR001W	<i>CIT3</i>	Citrate synthase	2.02	-1.40	1.41	-1.35	0	1
YOR393W	<i>ERR1</i>	Similarity to enolases	2.01	1.21	1.33	-1.15	4	0
YBR001C	<i>NTH2</i>	Neutral trehalase	2.01	1.25	1.14	1.62	1	0
<b>Stress response</b>								
YBL075C	<i>SSA3</i>	Heat-shock protein	9.64	1.21	1.99	1.75	0	2
YPL240C	<i>HSP82</i>	Heat-shock protein	2.85	1.25	1.05	1.86	2	1
YER096W	<i>SHC1</i>	Sporulation specific protein	2.47	1.14	1.41	1.36	1	2
YIL033C	<i>BCY1</i>	PKA, regulatory subunit	2.44	1.32	-1.36	1.13	0	0
YLR259C	<i>HSP60</i>	Heat-shock protein	2.42	-1.10	1.49	1.34	0	1
YPL203W	<i>TPK2</i>	PKA, catalytic subunit	2.22	-1.12	-1.18	1.54	1	0
YBL105C	<i>PKC1</i>	Ser/thr protein kinase	2.04	1.27	-1.13	-1.06	1	0
<b>Oxidative stress response</b>								
YIR038C	<i>GTT1</i>	Glutathione-S-transferase	3.17	1.02	1.16	1.41	3	0
YML004C	<i>GLO1</i>	Glyoxalase I	3.16	-1.13	-1.33	1.98	2	2
YMR250W	<i>GAD1</i>	Glutamate decarboxylase	3.11	1.31	-1.07	1.49	1	1
YOR031W	<i>CRS5</i>	Metallothionein	2.30	1.25	-1.04	2.03	3	2
YBR006W	<i>UGA2</i>	Succinate-semialdehyde dehydrogenase	2.20	-1.12	-1.42	1.38	0	0
YCR083W	<i>TRX3</i>	Mitochondrial thioredoxin protein	2.11	1.43	-1.13	1.30	1	0
YDR272W	<i>GLO2</i>	Glyoxalase II	2.10	1.21	-1.18	1.23	0	2
YJR048W	<i>CYC1</i>	Cytochrome-c isoform	2.05	1.11	1.69	-1.25	0	0
YJR104C	<i>SOD1</i>	Superoxide dismutase	1.92	-1.36	-1.34	1.01	2	1
YPL202C	<i>AFT2</i>	Transcription factor	1.80	-1.17	1.23	1.03	0	0
YNL241C	<i>ZWF1</i>	Glucose-6-phosphate dehydrogenase	1.78	-1.21	-1.01	-1.38	5	1
<b>Respiration</b>								
YLR327C		Putative ATPase stabilizing factor	3.35	1.20	2.00	3.43	3	0
YDR231C	<i>COX20</i>	Cytochrome oxidase assembly	2.79	1.16	1.07	2.57	1	0
YKL016C	<i>ATP7</i>	FO-ATP synthase d subunit	2.47	1.12	1.31	1.54	0	0
YLL009C	<i>COX17</i>	Cytochrome-c oxidase assembly	2.40	1.14	1.10	1.30	1	0
YNL052W	<i>COX5A</i>	Cytochrome-c oxidase chain	2.28	1.37	-1.07	1.20	0	0
YMR145C	<i>NDH1</i>	NADH dehydrogenase	2.15	1.12	1.37	1.37	4	1
YNL073W	<i>MSK1</i>	lysyl-tRNA synthetase	2.13	-1.64	-1.15	1.78	1	0
YBL045C	<i>COR1</i>	Ubiquinol-cytochrome-c reductase	2.12	1.25	1.49	1.79	2	1
YIL136W	<i>OM45</i>	Mitochondrial membrane protein	2.05	-1.06	1.49	1.40	3	0
YIL006W		Mitochondrial carrier family member	2.02	1.11	1.33	1.04	1	1

Table 1 RIM15-DEPENDENT TRANSCRIPTION AT THE DIAUXIC TRANSITION<sup>a</sup> (CONTINUED)

Lipid and fatty acid metabolism									
YDR313C	<i>PIB1</i>	PI(3)-phosphate binding protein	2.99	1.01	1.45	1.54	1	0	
YDR497C	<i>ITR1</i>	Major myo-inositol permease	2.98	-1.21	1.82	-1.24	0	0	
YKR067W	<i>GPT2</i>	Glycerol-3-phosphate O-acyltransferase	2.63	1.37	-1.02	2.22	2	0	
YIL160C	<i>POT1</i>	3-oxoacyl CoA thiolase	2.62	-1.01	1.08	1.57	0	0	
YAR035W	<i>YAT1</i>	Carnitine acetyltransferase	2.59	1.18	1.14	1.24	2	0	
YGR216C	<i>GPI1</i>	GPI anchor biosynthesis	2.58	1.20	1.24	1.36	1	1	
YDR173C	<i>ARG82</i>	Phosphatidylinositol kinase	2.33	1.31	1.59	1.79	0	1	
YJR073C	<i>OPI3</i>	Phospholipid methyltransferase	2.19	1.25	-1.14	1.93	1	0	
YDL078C	<i>MDH3</i>	Malate dehydrogenase	2.19	-1.26	1.09	1.55	1	1	
YEL020C		Putative oxalyl-CoA decarboxylase	2.04	1.05	1.09	1.20	0	1	
YKL020C	<i>SPT23</i>	Transcriptional activator	2.00	1.22	1.19	1.19	0	0	

<sup>a</sup>A change in mRNA levels was deemed significant based on the following criteria: the average fold change was consistent in duplicate experiments, the average fold change was >2-fold up in wild-type (W303-1A) cells entering the diauxic phase, and the corresponding fold change in *rim15Δ* (CDV115) cells was <1.5-fold up. Note: only gene clusters containing at least 7 genes that are either characterized or have a presumed function are represented. Of the selected ORFs, the corresponding average fold changes in *msn2 msn4* (PEY78) and *gis1Δ* (CDV116) cells are also shown. The number of STRE (AG<sub>4</sub>) and PDS (AG<sub>3</sub>AT) consensus sites within 1000 base pairs (bp) upstream of the transcription start sites of the corresponding ORFs is indicated (overlapping matches were allowed).

## RESULTS AND DISCUSSION

Since Rim15 appears to be the central regulator of G<sub>0</sub> entry, we decided to more precisely define its role by studying the genome-wide transcriptional profile of wild-type and *rim15Δ* mutant cells at the diauxic transition. We found five prominent classes of genes that were dependent on Rim15 for their proper induction at the diauxic shift. These classes represent genes whose products are involved in carbohydrate metabolism, general and oxidative stress response, respiration, and lipid and fatty acid metabolism (Table 1). Interestingly, most of these Rim15-dependent genes have previously been found to either depend on Msn2/4 for induction at the diauxic shift, and/or contain STREs in their promoter regions.<sup>8,31-33</sup> Moreover, of the 57 Rim15-dependent genes in Table 1, 39 have a perfect STRE consensus site within 1000 base pairs (bp) upstream of the transcription start site, which is in agreement with the notion that Rim15 may be implicated in the control of Msn2/4 function (see also refs. 18,34). In an alternative model, Rim15 may control these genes via Gis1, which can also bind both PDS and STRE-like sequences in vitro and possibly overlaps in vivo with Msn2/4 function.<sup>18,35,36</sup>

To explore further whether Rim15 may act through Msn2/4 and/or Gis1, we also studied the genome-wide transcriptional profile of *msn2 msn4* and *gis1Δ* cells at the diauxic transition. Surprisingly, we found that virtually the entire set of genes that required Rim15

for induction at the diauxic shift was included within the combined larger sets of Gis1 and Msn2/4-dependent genes (Fig. 1). Thus, while a fraction of the Gis1- and Msn2/4-dependent gene sets (27% and 40%, respectively) may be controlled independently of Rim15, Gis1 and Msn2/4 appear to mediate the entire Rim15-dependent transcriptional response at the diauxic shift. An attractive model that may explain these findings is that Rim15 regulates the establishment of physiological context-specific interactions of the general transcription machinery with Gis1, Msn2, and Msn4. This model is not without precedent<sup>37</sup> and is further supported by the observation that Rim15 exhibits two-hybrid interactions with two subunits of the general transcription factor TFIID (i.e., Taf25<sup>38</sup> and Taf1; CDV, unpublished observations). A second interesting aspect of our genome-wide expression analysis is that 95% of the Gis1-dependent genes are

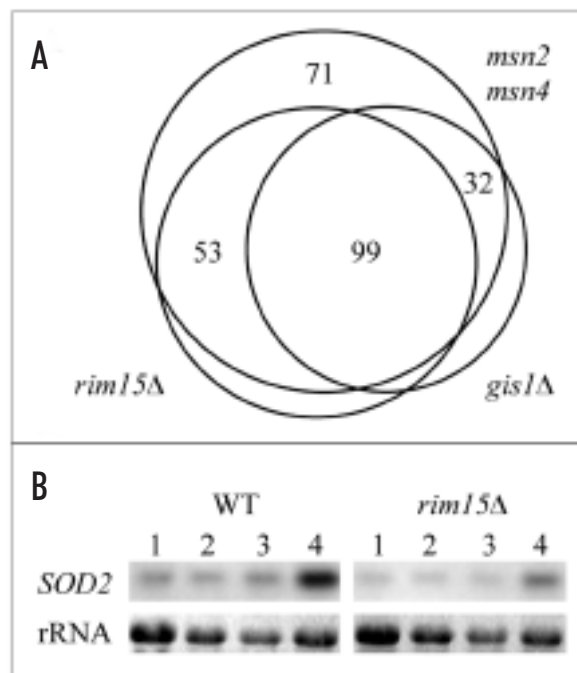


Figure 1. Induction of distinct sets of genes at the diauxic shift depends on Rim15, Gis1, and Msn2/4. (A) The Venn diagram illustrates the common genes affected by loss of either Rim15, Gis1, or Msn2/4. See "Materials and Methods" for further details. (B) Abundance of *SOD2* mRNA as wild-type (WT; KT1960) and *rim15Δ* (IP31) mutant cells enter the post-diauxic shift phase. Total RNAs were extracted from early exponential phase cells (lane 1; 2% external glucose), late exponential phase cells (lane 2; 1% external glucose), diauxic shift phase cells (lane 3; <0.1% external glucose), and post-diauxic shift phase cells (lane 4; <0.01% external glucose; 10 h following glucose exhaustion). Equal amounts of total RNA (5 μg) were probed with *SOD2* after electrophoresis and blotting. The application and transfer of equal amounts of RNA were verified by ethidium bromide staining.



included within the larger set of Msn2/4-dependent genes (Fig. 1). Since 55% of the promoters of these shared genes (Table 1 and data not shown) harbor either STREs or PDS elements, but not both elements combined, our data suggest that Gis1 and Msn2/4 not only functionally overlap *in vivo*, but also regulate transcription of a large set of genes in a cooperative manner.

The most surprising aspect of our genome-wide transcription analyses was that the Rim15 regulon comprises several gene clusters that are implicated in the adaptation to respiratory growth (Table 1). Importantly, Rim15 transcriptionally controls several classical oxidative stress genes, whose products are involved in antioxidant defense (e.g., *SOD1*, *TRX3*, and *CYC1*), regeneration of NADPH (e.g., *ZWF1*, *UGA2*, and *GAD1*), and detoxification of metabolic intermediates (e.g., *GLO1*, *GLO2*, and *GTT1*).<sup>11,12</sup> In addition, northern blot analyses revealed that the basal level of the mitochondrial catalase-encoding *SOD2* mRNA is lower in *rim15Δ* mutant cells, and that transcriptional induction of *SOD2*, which occurs later in the post-diauxic phase,<sup>39</sup> is strongly dependent on the presence of Rim15 (Fig. 1B). The dramatically reduced chronological life span of *rim15Δ* cells may therefore be due, at least in part, to the deficiency in induction of mechanisms that prevent oxidative damage. This suggestion is in line with the finding that the chronological life span

in yeast can be shortened by loss of either of the two superoxide dismutases Sod1 and Sod2.<sup>40</sup> Intriguingly, it was previously reported that life-span extension following downregulation of PKA or loss of Sch9 depends on the presence of Rim15 and/or Msn2/4.<sup>41,42</sup> Thus, together with our recent observation that Sch9 (like TOR) is required for nuclear exclusion and/or cytoplasmic retention of Rim15,<sup>28</sup> our present study supports a model in which Rim15 is capable of integrating signals from at least three nutrient-sensory kinases (TOR, PKA, and Sch9) to (directly or indirectly) control G<sub>0</sub> entry and longevity via its presumed downstream effectors Msn2, Msn4, and Gis1.

Oxidative stress responses are generally triggered by reactive oxygen species, which result from an increase in mitochondrial respiratory chain activity, known to occur at the diauxic transition.<sup>12</sup> Thus, an interesting question, in this context, is whether Rim15 may, in addition to nutrient signals, also integrate oxidative stress signals. While little is known of the mechanisms that sense oxygen and/or oxidative stress in yeast, bacteria are known to use PAS (Per-Arnt-Sim) domains in sensor modules of two-component systems to monitor parameters such as overall energy level, redox potential, and oxygen.<sup>22,23</sup> In some cases, bacterial PAS domains have been described to associate with defined ligands (e.g., FMN, FAD, and heme) and to serve as a

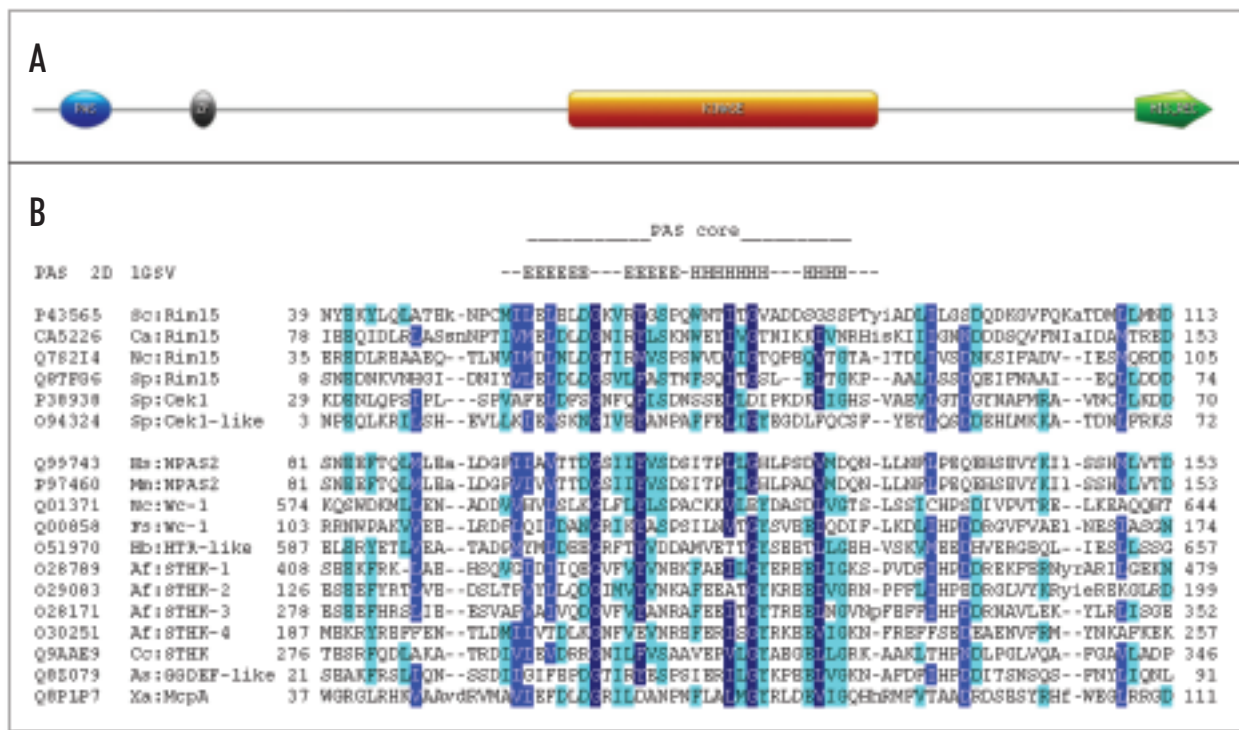


Figure 2. *S. cerevisiae* Rim15 represents a new member of the PAS kinase family. (A) Schematic diagram illustrating the domain architecture of the *S. cerevisiae* Rim15 protein. All domains are drawn approximately to scale. Rim15 belongs to a small group of conserved fungal proteins, which exhibit the same domain organization, including the N-terminal PAS (blue oval) and CCHC-type zinc finger (grey oval) domains, the central protein kinase domain (orange rectangle) that classifies Rim15 as a member of the conserved nuclear Dbf2-related (NDR) and large tumor suppressor (LATS) serine/threonine kinase subclasses of the protein kinase A, G, and C (AGC) class of kinases,<sup>49</sup> and a C-terminal receiver domain (green pentagon). (B) Alignment of the PAS domains found within the Rim15 family of fungal proteins with closely related, well-defined PAS motifs. The secondary structure of the core region, representing an extended  $\beta$ -strand (E) and an  $\alpha$ -helix (H), was deduced from the PDB entry (1GSV) and is indicated above the alignment. Amino acids that are conserved in more than 50%, 70% and 90% of the sequences are shown in light blue, blue, and dark blue, respectively. PAS domains were extracted from the *S. cerevisiae* Rim15 (P43565), *C. albicans* (<http://genolist.pasteur.fr/CandidaDB/>), *N. crassa* (Q78214), and *S. pombe* homologs (Q8TFG6), the *S. pombe* Cek1 (P38938) and Cek1-like protein (O94324), the *H. sapiens* (Q99743) and *M. musculus* (P97460) neuronal PAS domain protein 2, the *N. crassa* (Q01371) and *F. solani* (Q00858) white collar 1 protein, the *Halobacterium sp.* HTR-like protein (O51970), the *A. fulgidus* (O28789, O29083, O28171, O30251) and *C. crescentus* (Q9A9E9) sensory transducer histidine kinases, the *Anabaena sp.* GGDEF-like protein (Q8Z079), and the *X. axonopodis* McpA protein (Q8PLP7).

ligand-regulated switch, which exerts allosteric regulation in *cis* on histidine kinases.<sup>22,23</sup>

More recently, the genomes of yeast, flies, and mice were found to encode conserved serine/threonine kinases that may also be regulated in *cis* by one or both of two N-terminally located PAS domains.<sup>24,25</sup> Intriguingly, in this context, SMART<sup>43</sup> and PROSITE<sup>44</sup> databases identify a PAS domain in the Cek1 and Cek1-like proteins, which both represent *Schizosaccharomyces pombe* homologs of Rim15. Since the amino acid sequence relationships that define PAS-domains are often quite subtle (the conserved hydrophobic core of PAS domains encompasses approximately 30 amino acids), it is possible that a corresponding PAS domain in Rim15 may have escaped identification via conventional methods.<sup>45</sup>

To determine whether Rim15 may also harbor a N-terminal PAS domain, we used a combination of iterative database searches (initiated with an alignment of the PAS domains found in the *S. pombe* Cek1 and Cek1-like proteins) with generalized profiles and Hidden Markov Models (profile-HMMs).<sup>46,47</sup> Only sequences that matched a generalized profile or a profile-HMM with a significant score (E-value of <0.01) were used for subsequent iteration cycles. At the second cycle, we identified the *S. cerevisiae* Rim15 PAS domain (with an E-value of 10<sup>-3</sup>), as well as several other previously characterized PAS domains. The third and fourth cycles identified PAS domains of other Rim15 family members, while any of the following cycles were restricted to classical PAS domains (Fig. 2B). Taken together, these findings strongly suggest that Rim15 specifies in its amino-terminal part an evolutionarily conserved PAS domain, and therefore represents a new, distinct member of the PAS kinase family. Notably, the PAS domain of Rim15 appears closely related to the PAS domain in the neuronal PAS domain protein 2 (NPAS2; Fig. 2B), known to bind heme as a prosthetic group to function as a gas-regulated sensor.<sup>48</sup> Thus, by analogy, the Rim15-PAS domain may also function as a *cis* regulatory, ligand-activated switch that senses oxidative stress and/or the cellular redox status to properly control Rim15 protein kinase activity. Even though speculative at present, our suggestion leads to concrete predictions that can be addressed experimentally in the near future.

In summary, the results presented here, taken together with the previous observations that Rim15 integrates signals from both the TOR and PKA signaling pathways, enlarge our current view on the role of PAS kinases, and underline the notion that the cell-autonomous nutrient-sensory kinases Rim15, PKA, TOR, and Sch9 form a highly integrated and sophisticated network to control entry into G<sub>0</sub>. In yeast, glucose limitation at the diauxic shift is intimately linked with the onset of respiratory growth that is prone to dramatically change the cellular redox balance. Based on the Rim15-dependent readouts identified in this study and the discovery of an evolutionary conserved PAS domain in the N-terminal region of Rim15, we hypothesize that the Rim15 protein kinase may have evolved to integrate nutrient signals transduced via TOR, PKA, and possibly Sch9, and redox and/or oxidative stress signals to appropriately induce the transcriptional program that leads to cell survival in G<sub>0</sub> for an extended period of time.

## References

1. Werner-Washburne M, Braun E, Johnston GC, Singer RA. Stationary phase in the yeast *Saccharomyces cerevisiae*. Microbiol Rev 1993; 57:383-401.
2. Werner-Washburne M, Braun EL, Crawford ME, Peck VM. Stationary phase in *Saccharomyces cerevisiae*. Mol Microbiol 1996; 19:1159-66.
3. Herman PK. Stationary phase in yeast. Curr Opin Microbiol 2002; 5:602-7.
4. Bitterman KJ, Medvedik O, Sinclair DA. Longevity regulation in *Saccharomyces cerevisiae*: Linking metabolism, genome stability, and heterochromatin. Microbiol Mol Biol Rev 2003; 67:376-99.
5. Lillie SH, Pringle JR. Reserve carbohydrate metabolism in *Saccharomyces cerevisiae*: Responses to nutrient limitation. J Bacteriol 1980; 143:1384-94.
6. Mager WH, De Kruijff AJ. Stress-induced transcriptional activation. Microbiol Rev 1995; 59:506-31.
7. Ruis H, Schüller C. Stress signalling in yeast. Bioassays 1995; 17:959-65.
8. Boy-Marcotte E, Perrot M, Bussereau F, Boucherie H, Jacquet M. Msn2p and Msn4p control a large number of genes induced at the diauxic transition which are repressed by cyclic AMP in *Saccharomyces cerevisiae*. J Bacteriol 1998; 180:1044-52.
9. Thevelein JM, de Winde JH. Novel sensing mechanisms and targets for the cAMP-protein kinase A pathway in the yeast *Saccharomyces cerevisiae*. Mol Microbiol 1999; 33:904-18.
10. Estruch F. Stress-controlled transcription factors, stress-induced genes and stress tolerance in budding yeast. FEMS Microbiol Rev 2000; 24:469-86.
11. Jamieson DJ. Oxidative stress response of the yeast *Saccharomyces cerevisiae*. Yeast 1998; 14:1511-27.
12. Costa V, Moradas-Ferreira P. Oxidative stress and signal transduction in *Saccharomyces cerevisiae*: Insights into ageing, apoptosis and diseases. Mol Asp Med 2001; 22:217-46.
13. Braun EL, Fuge BE, Padilla PA, Werner-Washburne M. A stationary-phase gene in *Saccharomyces cerevisiae* is a member of a novel, highly conserved gene family. J Bacteriol 1996; 178:6865-72.
14. Padilla PA, Fuge EK, Crawford ME, Errett A, Werner-Washburne M. The highly conserved, coregulated *SNO* and *SNZ* gene families in *Saccharomyces cerevisiae* respond to nutrient limitation. J Bacteriol 1998; 180:5718-26.
15. Rhode J, Heitman J, Cardenas ME. The TOR kinases link nutrient sensing to cell growth. J Biol Chem 2001; 276:9583-6.
16. Jacinto E, Hall MN. TOR signalling in bugs, brain and brawn. Nat Rev Mol Cell Biol 2003; 4:117-26.
17. Reinders A, Bürckert N, Boller T, Wiemken A, De Virgilio C. *Saccharomyces cerevisiae* cAMP-dependent protein kinase controls entry into stationary phase through the Rim15p protein kinase. Genes Dev 1998; 12:2943-55.
18. Pedrucci I, Bürckert N, Egger P, De Virgilio C. *Saccharomyces cerevisiae* Ras/cAMP pathway controls post-diauxic shift element-dependent transcription through the zinc finger protein Gis1. EMBO J 2000; 19:2569-97.
19. Görner W, Durchschlag E, Wolf J, Brown EL, Ammerer G, Ruis H, et al. Acute glucose starvation activates the nuclear localization signal of a stress-specific yeast transcription factor. EMBO J 2002; 21:135-44.
20. Schmelzle T, Beck T, Martin DE, Hall MN. Activation of the Ras/cyclic AMP pathway suppresses a TOR deficiency in yeast. Mol Cell Biol 2004; 24:338-51.
21. Griffioen G, Anghileri P, Imre E, Baroni MD, Ruis H. Nutritional control of nucleocytoplasmic localization of cAMP-dependent protein kinase catalytic and regulatory subunits in *Saccharomyces cerevisiae*. J Biol Chem 2000; 275:1449-56.
22. Taylor BL, Zhulin IB. PAS domains: Internal sensors of oxygen, redox potential, and light. Microbiol Mol Biol Rev 1999; 63:479-506.
23. Gilles-Gonzales M-A, Gonzales G. Signal transduction by heme-containing PAS-domain proteins. J Appl Physiol 2004; 96:774-83.
24. Rutter J, Michnoff CH, Harper SM, Gardner KH, McKnight SL. PAS kinase: An evolutionary conserved PAS domain-regulated serine/threonine kinase. Proc Natl Acad Sci USA 2001; 98:8991-6.
25. Rutter J, Probst BL, McKnight SL. Coordinate regulation of sugar flux and translation by PAS kinase. Cell 2002; 111:17-28.
26. Amezcua CA, Harper SM, Rutter J, Gardner KH. Structure and interactions of PAS kinase N-terminal PAS domain: Model for intramolecular kinase regulation. Structure 2002; 10:1349-61.
27. Martínez-Pastor MT, Marchler G, Schüller C, Marchler-Bauer A, Ruis H, Estruch F. The *Saccharomyces cerevisiae* zinc finger proteins Msn2p and Msn4p are required for transcriptional induction through the stress-response element (STRE). EMBO J 1996; 15:2227-35.
28. Pedrucci I, Dubouloz F, Cameron E, Wanke V, Roosen J, Winderickx J, et al. TOR and PKA signaling pathways converge on the protein kinase Rim15 to control entry into G<sub>0</sub>. Mol Cell 2003; 12:1607-13.
29. Longtine MS, McKenzie A 3rd, DeMarini DJ, Shah NG, Wach A, Brachat A, et al. Additional modules for versatile and economical PCR-based gene deletion and modification in *Saccharomyces cerevisiae*. Yeast 1998; 14:953-61.
30. Sherman F. In: Guide to Yeast Genetics and Molecular Biology. eds. Guthrie C, Fink G R. Academic San Diego, 1991:3-21.
31. DeRisi JL, Iyer VR, Brown PO. Exploring the metabolic and genetic control of gene expression on a genomic scale. Science 1997; 278:680-6.
32. Gasch AP, Spellman PT, Kao CM, Carmel-Harel O, Eisen MB, Storz G, et al. Genomic expression programs in the response of yeast cells to environmental changes. Mol Biol Cell 2000; 11:4241-57.
33. Causton HC, Ren B, Koh SS, Harbison CT, Kanin E, Jennings EG, et al. Remodeling of yeast genome expression in response to environmental changes. Mol Biol Cell 2001; 12:323-37.
34. Lensen E, Oberholzer U, Labarre J, De Virgilio C, Collart MA. *Saccharomyces cerevisiae* Ccr4-Not complex contributes to the control of Msn2p-dependent transcription by the Ras/cAMP pathway. Mol Microbiol 2002; 43:1023-37.
35. Treger JM, Schmitt AP, Simon JR, McEntee K. Transcriptional factor mutations reveal regulatory complexities of heat shock and newly identified stress genes in *Saccharomyces cerevisiae*. J Biol Chem 1998; 273:26875-9.

36. Jang YK, Wang L, Sancar GB. *RPH1* and *GIS1* are damage-responsive repressors of *PHR1*. *Mol Cell Biol* 1999; 19:7630-8.
37. Mencía M, Moqtaderi Z, Geisberg JV, Kuras L, Struhl K. Activator-specific recruitment of TFIID and regulation of ribosomal protein genes in yeast. *Mol Cell* 2002; 9:823-33.
38. Kirchner J, Sanders SL, Klebanow E, Weil PA. Molecular genetic dissection of *TAF25*, an essential yeast encoding a subunit shared by TFIID and SAGA multiprotein transcription factors. *Mol Cell Biol* 2001; 21:6668-80.
39. Flattery-O'Brien JA, Grant CM, Dawes IW. Stationary-phase regulation of the *Saccharomyces cerevisiae* *SOD2* gene is dependent on additive effects of HAP2/3/4/5- and STRE-binding elements. *Mol Microbiol* 1997; 23:303-12.
40. Longo VD, Gralla EB, Valentine JS. Superoxide dismutase activity is essential for stationary phase survival in *Saccharomyces cerevisiae*. *J Biol Chem* 1996; 271:12275-80.
41. Fabrizio P, Pozza F, Pletcher SD, Gendron CM, Longo VD. Regulation of longevity and stress resistance by Sch9 in yeast. *Science* 2001; 292:288-90.
42. Fabrizio P, Liou L-L, Moy VN, Diaspro A, Valentine JS, Gralla EB, et al. *SOD2* functions downstream of Sch9 to extend longevity in yeast. *Genetics* 2003; 163:35-46.
43. Letunic I, Copley RR, Schmidt S, Ciccarelli FD, Doerks T, Schultz J, et al. SMART 4.0: Towards genomic data integration. *Nucleic Acids Res* 2004; 32:D142-4.
44. Hulo N, Sigrist CJA, Le Saux V, Langendijk-Genevaux PS, Bordoli L, Gattiker A, et al. Recent improvements to the PROSITE database. *Nucleic Acids Res* 2004; 32:D134-7.
45. Ponting CP, Aravind L. PAS: A multifunctional domain family comes to light. *Curr Biol* 1997; 7:R674-7.
46. Bucher P, Karplus K, Moeri N, Hofmann K. A flexible motif search technique based on generalized profiles. *Comput Chem* 1996; 20:3-23.
47. Eddy SR. Profile hidden Markov models. *Bioinformatics* 1998; 14:755-63.
48. Dioum EM, Rutter J, Tuckerman JR, Gonzales G, Gilles-Gonzales M-A, McKnight SL. NPAS2: A gas-responsive transcription factor. *Science* 2002; 298:2385-7.
49. Tamaskovic R, Bichsel SJ, Hemmings BA. NDR family of AGC kinases – essential regulators of the cell cycle and morphogenesis. *FEBS Lett* 2003; 546:73-80.